Line broadening studies for Cr^{3+} pairs and single ions in different oxide lattices

2000 J. Phys.: Condens. Matter 12 8607

(http://iopscience.iop.org/0953-8984/12/40/305)

J. Phys.: Condens. Matter **12** (2000) 8607–8615. Printed in the UK PII: S0953-8984(00)11662-5

Line broadening studies for Cr^{3+} pairs and single ions in different oxide lattices

A P Vink†, M A de Bruin and A Meijerink

Department of Condensed Matter, Debye Institute, PO Box 80 000, 3508 TA Utrecht, The Netherlands

Received 7 February 2000, in final form 3 July 2000

Abstract. The electron–phonon coupling for Cr^{3+} in different oxide host lattices (MgO, α-Al_2O_3 and $LaAlO_3$) was probed by performing temperature dependent line broadening measurements for zero-phonon emission lines of single ions and exchange coupled pairs. No differences in electron–phonon coupling were found comparing the results for pairs and single ions in α-Al_2O_3 (3NN and 4NN pairs) and $LaAlO_3$ (NN pairs). In Cr^{3+} doped MgO (Cr^{3+}–V_{Mg}–Cr^{3+} pairs), it was found that the electron–phonon coupling strength parameter $\bar{\alpha}$ is larger for the pairs than for the isolated Cr^{3+} ions. This is probably due to changes in the surroundings of Cr^{3+} by local charge compensation by a magnesium vacancy, and not to interaction between the Cr^{3+} ions.

1. Introduction

The electron–phonon coupling for the 4f–4f transitions of the lanthanides has been studied intensively [1–10]. It was found that the coupling is high at the beginning of the lanthanide series, decreases in the middle and then increases at the end of the series [3]. Also a dependence of electron–phonon coupling on the host lattice was found; in covalent host lattices a stronger electron–phonon coupling is observed [4].

The dependence of electron–phonon coupling on the concentration of the rare-earth dopant ion was also reported [11–16]. As an explanation, difference models were suggested (for example super-exchange of holes between Eu^{3+} ions [11, 13]) and exchange of virtual phonons between coupled Pr^{3+} ions in pairs [14, 15]. Later, it was shown that in fact the observed concentration enhancement of vibronic lines is due to an artefact [17].

The electron–phonon coupling of 3d transition metal ions has not been studied to the same extent as for lanthanides. Although a lot of work has been done on the electron–phonon coupling of the transition metal ion Cr^{3+} ($3d^3$) [18–21], the influence of dopant concentration on the electron–phonon coupling was never investigated. The electron–phonon coupling of the transition metal ions is much stronger than for the lanthanides because the 3d electrons of the transitions metal ions are not shielded from their surroundings by outer filled shells, as is the case for the 4f electrons of the lanthanides. Therefore the interaction with the surround ligands is stronger for 3d transition metal ions [3, 4]. If there is an increase in the electron–phonon coupling strength due to (super)exchange interaction between ions in pairs, as suggested in the theoretical models in [11, 14–16], a stronger electron–phonon coupling could be expected for pairs of transition metal ions, even though no effect is observed for the weakly interacting lanthanide ions.

† Coresponding author.

This paper deals with investigations on the electron–phonon coupling for single Cr^{3+} ions and Cr^{3+} pairs in various host lattices. The electron–phonon coupling is probed by temperature dependent line broadening measurement. Other methods to probe the electron–phonon coupling strength such as measuring the transition probabilities for vibronic lines or multi-phonon relaxation rates cannot be used: selective excitation of single Cr^{3+} ions or Cr^{3+} pair sites is not possible. Due to energy transfer processes between sites, the emission spectra always contain contributions for different sites and the vibronic transition probabilities for one type of Cr^{3+} site cannot be determined. Previous studies [1, 4] however, have shown that the variation in electron–phonon coupling strength affects the different types of manifestations of electron–phonon coupling in similar way, i.e. a stronger coupling gives a more pronounced line broadening, more intense vibronic sidebands and faster multi-phonon relaxation. Thus the results on the electron–phonon coupling strength probed by temperature dependent line broadening studies have a more general significance. To study the phonon induced line broadening host lattices were chosen in which the Cr^{3+}-ion shows sharp $^2E \rightarrow {}^4A_2$ emission lines, for both the single ions and the pairs. Due to the narrow (homogeneous) linewidth of this transition at low temperatures, the electron–phonon coupling strength can be probed by measuring line broadening at higher temperatures due to phonon induced dephasing processes. Here, line broadening measurements for single ions and pairs of Cr^{3+} in the host lattices MgO, α-Al_2O_3 and $LaAlO_3$ are reported.

The most intense pair lines in the luminescence spectra of Cr^{3+} doped into MgO originate from charge compensation, which is needed because a trivalent ion (Cr^{3+}) is incorporated on a divalent (Mg^{2+}) site [22, 23]. Besides the single ion-emission of Cr^{3+} at a wavelength of 698 nm (R-line), pair-emission originating from Cr^{3+}–V_{Mg}–Cr^{3+} centres can be observed at 703.9 and 699.2 nm. These lines are called the N_2 lines (for more details, see [22, 23]). The Cr^{3+}–Cr^{3+} distance in this pair is 3.9 Å [24].

In α-Al_2O_3:Cr^{3+}, better known as ruby, the most intense pair lines correspond to luminescence of third- (3NN) and fourth-nearest-neighbours (4NN) Cr^{3+} pairs [25]. Because of the exchange interaction, the pair spectra show splitting and from the splitting the positions of the spin states can be determined. Due to magnetic coupling between the Cr^{3+} ions, states with different total magnetic spin moment occur. The ground state with $S = 3/2$ results in coupled states with total magnetic spin moment of 3, 2, 1 and 0. In a pair with one Cr^{3+} ion in the excited ^2E state ($S = 1/2$) total magnetic moments of 1 and 2 are possible. Transitions between states with the same total magnetic spin moment are partially spin-allowed. Transitions between pair states are indicated by the total magnetic spin moments, for example, $2 \rightarrow 2$. Here the numbers indicate the total magnetic spin moment of the coupled pair. For anti-ferromagnetic coupling the lowest total magnetic spin moment corresponds to the lowest energy state, while for ferromagnetic coupling the highest total magnetic spin moment is the lowest energy pair state. The strongest pair emission lines in ruby correspond to the $2 \rightarrow 2$ transition of the 3NN site ($\lambda_{em} = 704.3$ nm, called N_2) and the $1 \rightarrow 1$ transition of the 4NN site ($\lambda_{em} = 701$ nm, called N_1) [25]. The 3NN pairs have an anti-ferromagnetic (AFM) interaction (J is about -5.6 cm^{-1}) and the 4NN have a ferromagnetic (FM) interaction (J is about 3.5 cm^{-1}) [25]. The single ion shows emission at 693.6 (R_1-line) and 692.2 nm (R_2-line) [25]. The Cr^{3+}–Cr^{3+} pair distances are 3.19 Å for the 3NN and 3.50 Å for the 4NN [26].

In Cr^{3+}-doped $LaAlO_3$ the most intense pair-emission can be found at wavelength of 748 nm and is assigned to the $2 \rightarrow 2$ transition of the exchange coupled nearest neighbour (NN) Cr^{3+} pair [27]. Emission from the single Cr^{3+} ions (R-lines) is situated at 734 (R_1) and 733.7 nm (R_2) [28]. The Cr^3–Cr^{3+} distance of the NN pairs is 3.78 Å [27]. Besides NN Cr^{3+}-pair emissions, also emission from next-nearest-neighbour pairs was measured [28], but will not be discussed here.

To study the influence of pair formation on the electron–phonon coupling strength of Cr^{3+}, the electron–phonon coupling for Cr^{3+}-doped MgO (R, N_2) α-Al_2O_3 (R_1, N_1 and N_2) and $LaAlO_3$ (R_1 and NN pair line) was probed by measuring temperature dependent line broadening.

2. Theory

The electron–phonon coupling is the interaction between electronic states of a dopant and host lattice vibrations (phonons). The electron–phonon coupling manifests itself in a number of spectroscopic properties such as non-radiative decay, vibronics near a zero phonon line and increase of linewidth and line shift to lower or higher energies at increasing temperature [2, 29]. In this paper only line broadening will be discussed.

The uncertainty principle of Heisenberg, $\Delta E\tau \geqslant \hbar$ shows that the uncertainty in the energy of a state (ΔE) increases as the life time (τ) decreases. When the temperature is increased, the life time τ decreases and therefore the uncertainty in the energy increases, resulting in a larger (homogeneous) spectral linewidth [2]. The total linewidth $E(T)$ also contains contributions from the inhomogeneous linewidth, which is caused by strains and defects in the lattice and is (in good approximation) temperature independent. The temperature dependent part involves the life-time broadening due to several one-phonon and two-phonon dephasing processes [2, 29]:

$$E(T) = E^{Inh} + E^{Hom}(T) = E^{Inh} + E^{Orbach} + E^{D}_{Abs} + E^{D}_{Em} + E^{Raman}. \qquad (1)$$

The contribution of the direct one-phonon absorption $E^{D}_{Abs}(T)$ and emission $E^{D}_{Em}(T)$ process is usually small and can be neglected at all but the lowest temperatures [2, 6, 29]. The contribution of Orbach two-phonon process $E^{Orbach}(T)$ can be important if a (partially) allowed one-phonon transition to a higher level is possible. In the case of Cr^{3+} a significant contribution of the Orbach process is expected if the $^4T_2$ level is situated just above the ^2E level. In the presently studied host lattices the energy difference between the ^2E level and the $^4T_2$ level is about 2000 cm^{-1} (MgO and Al_2O_3) up to 3400 cm^{-1} ($LaAlO_3$) which is more than the maximum phonon energy (700 cm^{-1} in aluminates). Thus in good approximation the line broadening can befitted to an inhomogeneous part and a temperature dependent part which describes line broadening due to the Raman two-phonon process, as is shown in equation (2) [2, 6, 29].

$$E(T) = E^{Inh} + \bar{\alpha}\left(\frac{T}{T_D}\right)^7 \int_0^{\frac{T_D}{T}} \frac{x^6 e^x}{(e^x - 1)^2}\,\mathrm{d}x \qquad (2)$$

The x in equation (2) is equal to $x = \hbar\omega/kT$ [2]. The electron–phonon coupling parameter $\bar{\alpha}$ can be determined by fitting the linewidth as a function of temperature to equation (2), taking the inhomogeneous linewidth E^{Inh} and the Debye temperature T_D as fixed parameters.

The Debye temperature T_D is a measure for the effective maximum phonon energy. In the Debye model the phonon density of states increases proportional to ω^2 and then drops to zero at the phonon cut-off frequency $\omega_{Cut\text{-}off}$. The Debye temperature can be calculated from $\omega_{Cut\text{-}off}$ by using: $T_D = \hbar\omega_{Cut\text{-}off}/k$ [2]. The Debye temperature used for the host lattices α-Al_2O_3 (760 K) and MgO (650 K) were taken from literature [18, 19], whereas the values for the host lattice $LaAlO_3$ (550 K) was determined from the vibronic sideband spectrum. The Debye temperature has been estimated by using the phonon frequency where the intensity in the vibronic spectrum is at a maximum (maximum phonon density of states) as $\omega_{Cut\text{-}off}$ and the corresponding T_D can then be calculated. This procedure works better than using the (considerably higher) real phonon cut-off frequency which would overestimate the phonon density of states for high-energy vibrations (see also [30]).

3. Experimental details

The MgO:Cr^{3+} powder was synthesized by firing an intimate mixture of the starting materials $(MgCO_3)_4Mg(OH)_2{\cdot}5H_2O$ and Cr_2O_3 under N_2 atmosphere for 5 hours at 1200 °C. α-Al_2O_3:Cr^{3+} was prepared by taking $NH_4Al(SO_4)_2{\cdot}12H_2O$ and Cr_2O_3 as starting materials and firing 1200 °C under N_2 for ten hours. $LaAlO_3$:Cr^{3+} was synthesized by mixing $NH_4Al(SO_4)_2 \cdot 12H_2O$, La_2O_3 and Cr_2O_3 (in a planetary ball mill) and firing the mixture under N_2 for three hours at 1000 °C and five hours at 1500 °C. The Cr^{3+} concentration was 1 mol% in MgO and 2 mol% in α-Al_2O_3 and $LaAlO_3$ with respect to Al^{3+} of Mg^{2+} (based on the starting materials). The actual Cr^{3+} concentration incorporated in the various lattices may be slightly different. For the present investigations, this is not important.

The purity of the samples was checked using a Perkin Elmer Lambda UV/VIS Spectrophotometer (optical) and on a Phillips PW 1729 x-ray diffractometer using Cu Kα-radiation (single crystalline phase). The diffuse reflection spectra showed that in all three cases Cr^{3+} was incorporated. No evidence for a second crystalline phase was found in the x-ray powder diffraction pattern.

The temperature dependent line broadening measurements were performed using a frequency doubled Quanta-Ray Nd:YAG-laser (532 nm) as an excitation source. Emission spectra were measured using a 1.26 m Spex 1269 monochromator and a cooled Hamamatsu R928 photomultiplier tube. More details on the set-up can be found in [31]. Data collection and processing was done using the Measure4 program developed by Dr U Oetliker.

4. Results

The emission spectrum of Cr^{3+} doped MgO is shown in figure 1. The R-line is situated at $\lambda_{em} = 698.2$ nm and the strongest Cr^{3+}–V_{Mg}–Cr^{3+} pair emission can be found at 703.9 nm (N_2). The N_2-emission shows strong overlap with the N_1-emission which is assigned to the Mg^{2+}–V_{Mg}–Cr^{3+} site [22, 23]. However, it was possible to determine the line broadening of the N_2 and R-line. The full width at half maximum (FWHM) as a function of temperature is shown in figure 2 with a fit to equation (2).

The emission spectrum of Cr^{3+} doped α-Al_2O_3 at $T = 7$ K is shown in figure 3. The R_1-line at $\lambda_{em} = 693.1$ nm can be clearly observed as well as the most intense pair emissions: the $1 \rightarrow 1$ transition of the 4NN pair at $\lambda_{em} = 700.8$ nm (N_1) and $2 \rightarrow 2$ of the 3NN at $\lambda_{em} = 704.1$ nm (N_2). More pair emission lines due to transitions between other spin states of the 3NN and 4NN pairs can also be observed (see assignment in figure 3). The presently observed wavelengths differ about 0.3 nm from values found in the literature and are probably due to a small error in the calibration of the monochromator. The FWHM (in cm^{-1}) of the emission lines between 4 K and room temperature are in figure 4 with a fit to equation (2).

The emission spectrum of $LaAlO_3$:Cr^{3+} at $T = 7$ K can be found in figure 5 and shows the R-line emissions at 733.8 (R_2) and 733.5 (R_1) nm. Besides the R-lines different pair emission lines are also observed. The $2 \rightarrow 2$ emission line from the NN pair at $\lambda_m = 748$ nm is the most intense. The other emissions are attributed to transitions between other spin states of the NN-pair and vibronic lines. The energy difference between the two R-lines is small and especially at higher temperatures, it was difficult to separate the R-lines. Still, the FWHM could be determined for the R_1 and the NN-pair at temperatures between 4 and 200 K. Due to the poor separation of the R_1 from the R_2 at higher temperatures and the quenching of the NN pair line, reliable results could not be obtained above 200 K. In figure 6, the FWHM in cm^{-1} at elevated temperatures (up to $T = 200$ K) are shown together with the fit to equation (2).

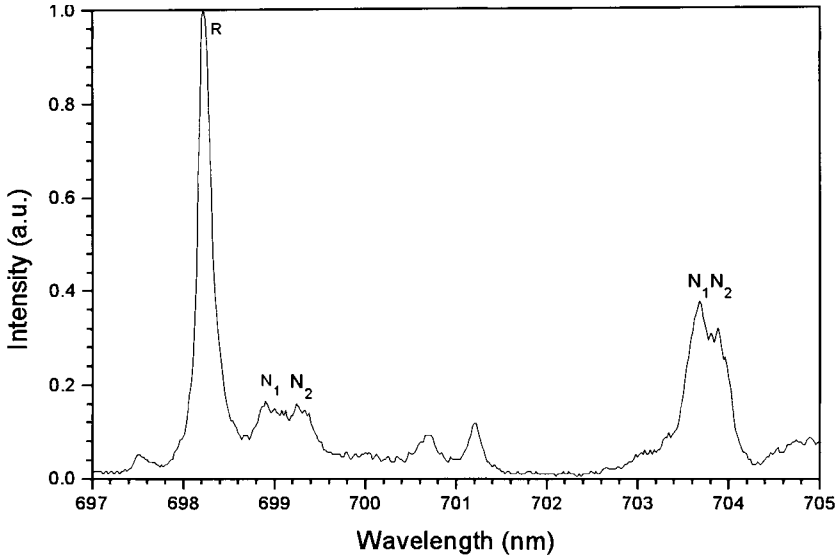

Figure 1. Emission spectrum ($\lambda_{exc} = 532$ nm) of MgO:Cr^{3+} at $T = 4$ K showing the R-line and the four pair emission lines (N_1 and N_2).

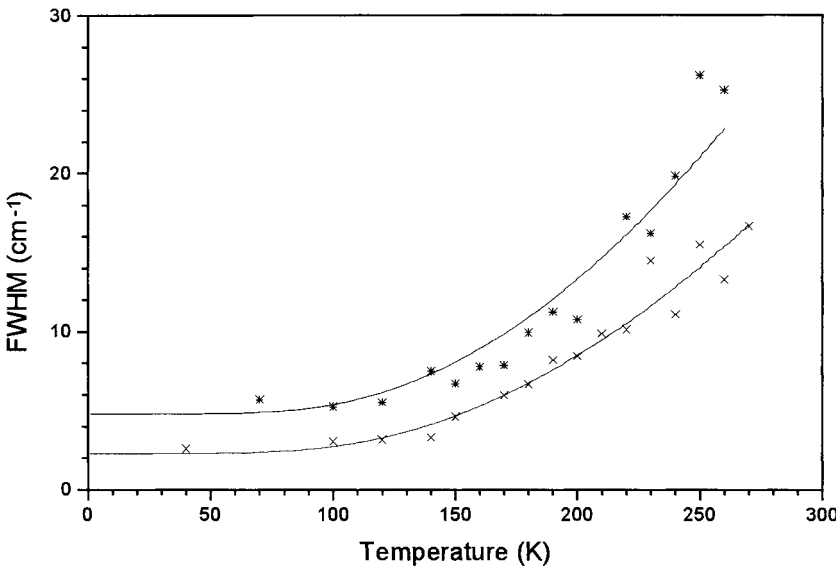

Figure 2. Linewidth (FWHM) of the R ($\times$) and N_2-line ($*$) in MgO:Cr^{3+} as a function of temperature, showing the data points and a fit to equation (2) (drawn line) using $T_D = 650$ K.

5. Discussion

The electron–phonon coupling parameters $\bar{\alpha}$ determined for the single Cr^{3+} ions and the Cr^{3+} pairs for the different host lattices are shown in table 1. For Cr^{3+} in Al_2O_3 and $LaAlO_3$, the electron–phonon coupling parameters $\bar{\alpha}$ are similar for the single ions and the different types of pairs. Simulations for which the value of $\bar{\alpha}$ was chosen to be 50 cm^{-1} higher or lower than

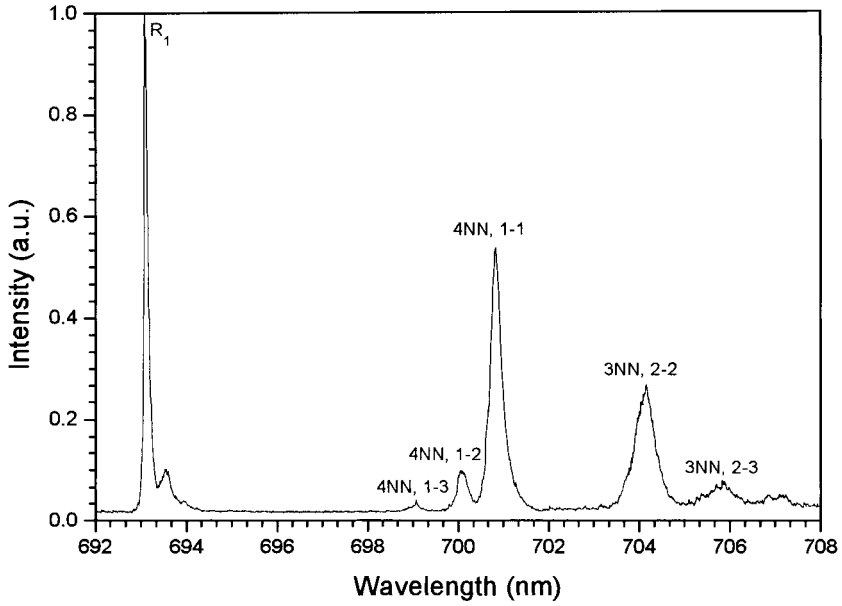

Figure 3. Emission spectrum ($\lambda_{exc} = 532$ nm) of α-Al_2O_3:Cr^{3+} at $T = 4$ K showing the R_1-line and different emission lines of the 3NN and 4NN pairs. The two most intense pair lines are the N_1 (3NN) and N_2 (4NN).

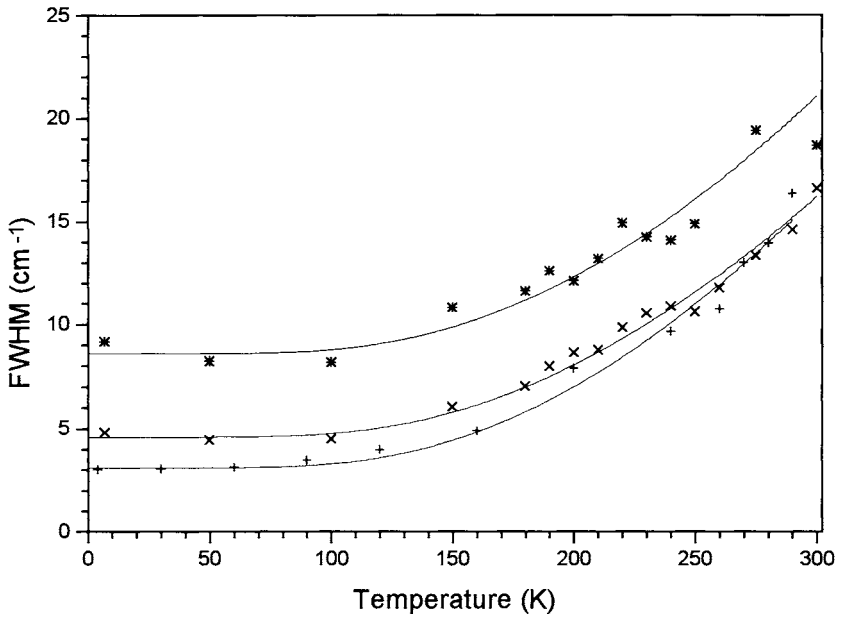

Figure 4. Linewidth (FWHM) of the R_1 (+), N_1 ($*$) and N_2-lines ($\times$) of α-Al_2O_3:Cr^{3+} as a function of temperature, showing the data points and the fit to equation (2) using $T_D = 760$ K.

the values obtained from the fits to equation (2) still give a reasonably good agreement with the experimentally observed values. Thus the differences found for $\bar{\alpha}$ from the fits to equation (2)

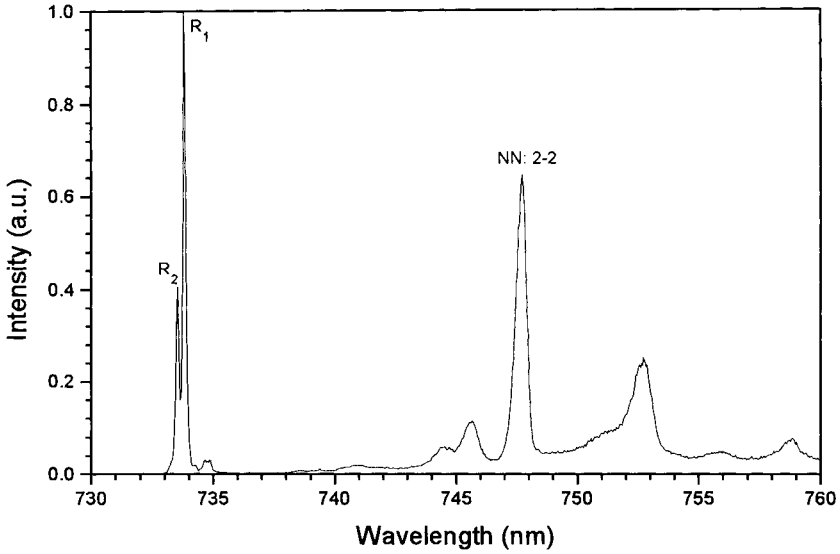

Figure 5. Emission spectrum ($\lambda_{exc} = 532$ nm) of $LaAlO_3$:Cr^{3+} at $T = 7$ K showing both R-lines and the most intense emission line of the NN Cr^{3+} pair.

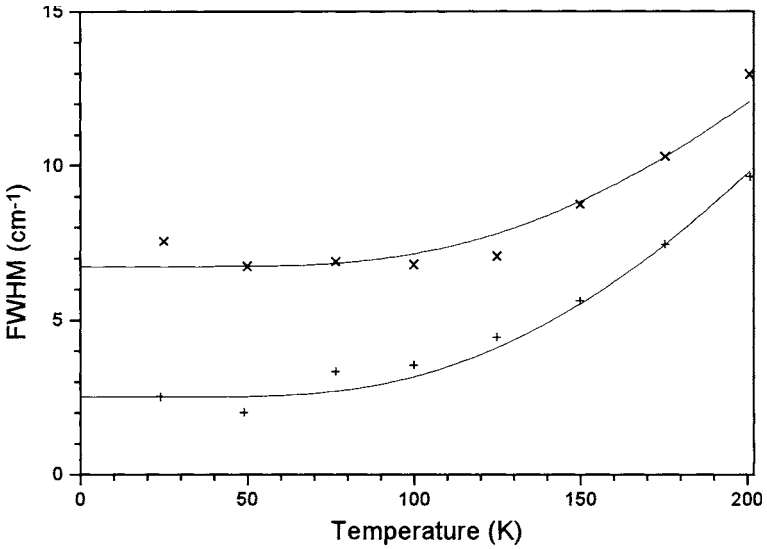

Figure 6. Linewidth (FWHM) of the R_1 (+) and the $2 \rightarrow 2$ NN-pair ($\times$) in $LaAlO_3$:Cr^{3+} as a function of temperature, showing the data points and a fit to equation (2) using $T_D = 550$ K.

for single Cr^{3+} ions and Cr^{3+} pairs are within experimental error for Cr^{3+} in Al_2O_3 and $LaAlO_3$. This shows that, in spite of the strong exchange coupling, the coupling with lattice vibrations is not affected. The values for the electron–phonon coupling parameters is around 500 cm^{-1}, which is typically observed for the $^2E \rightarrow {}^4A_2$ emission in oxides [18, 19].

For Cr^{3+} in MgO, the pair site shows larger values for the electron–phonon coupling parameter $\tilde{\alpha}$. Probably, this larger value is not due to exchange coupling between two Cr^{3+} ions. In MgO the Cr^{3+} pair sites are Cr^{3+}–V_{Mg}–Cr^{3+} sites. In this site two Cr^{3+} on Mg^{2+} sites

Table 1. The electron–phonon coupling parameter $\bar{\alpha}$ determined from temperature dependent line broadening measurements for emission from both single Cr^{3+} ions (R lines) and Cr^{3+} pairs (N lines).

Host lattice	Site	$\bar{\alpha}$ (cm^{-1})	E^{Inh} (cm^{-1})
MgO	R	580	2.3
$T_D = 650$ K	N_2	800	4.8
α-Al_2O_3	R_1	605	3.1
$T_D = 760$ K	N_1	575	8.6
	N_2	535	4.6
$LaAlO_3$	R_1	416	2.5
$T_D = 550$ K	NN	391	6.7

are charge compensated by a Mg vacancy. The presence of a vacancy between two Cr^{3+} ions can be expected to change the coupling with lattice vibrations and also the energy of local vibrational modes can be expected to be lower due to weakening of bonds by the present of a vacancy [32].

It would be interesting to measure the vibronic spectrum for the Cr^{3+}–V_{Mg}–Cr^{3+} site selectively to probe changes in the vibronic spectrum related to the magnesium vacancy. Selective excitation of the Cr^{3+}–V_{Mg}–Cr^{3+} turned out to be impossible. It could also be interesting to measure the influence of a local vacancy on the vibronic coupling of a lanthanide ion. Also a small increase of the electron–phonon coupling for a lanthanide next to a vacancy is expected. A possibility to study this effect would be in $CsCdBr_3$:Ln^{3+} where luminescence from single Ln^{3+} ions and from Ln^{3+}–V_{Cd}–Ln^{3+} sites have been observed, similar to the situation for Cr^{3+} in MgO [33].

6. Conclusions

The electron–phonon coupling parameter $\bar{\alpha}$ was measured for the $^2E \rightarrow {}^4A_2$-emission of Cr^{3+} pairs and single Cr^{3+} ions in MgO, α-Al_2O_3 and $LaAlO_3$. Temperature dependent line broadening measurements reveal no differences in electron–phonon coupling strength for pairs and single ion sites for Cr^{3+} in α-Al_2O_3 (3NN and 4NN-pairs) and $LaAlO_3$ (NN-pairs). This indicates that exchange coupling between the Cr^{3+} ions does not affect the electron–phonon coupling strength. In MgO (Cr^{3+}–V_{Mg}–Cr^{3+}-pairs) a higher $\bar{\alpha}$ value was found for the pairs compared to the single Cr^{3+} ions. This is probably due to changes in the surroundings of Cr^{3+} by local charge compensation and not to interaction between the Cr^{3+} ions.

References

[1] Hellwege K M 1941 *Ann. Phys.* **40** 529
[2] Ellens A, Andres H, Meijerink A and Blasse G 1997 *Phys. Rev.* B **55** 173
[3] Ellens A, Andres H, ter Heerdt M L H, Wegh R T, Meijerink A and Blasse G 1997 *Phys. Rev.* B **55** 180
[4] Meijerink A, Blasse G, Sytsma J, de Mello Donegá C and Ellens A 1996 *Acta. Phys. Pol.* A **90** 109
[5] Yen W M, Scott W C and Schawlow A L 1964 *Phys. Rev.* A **136** 271
[6] Kushida T 1969 *Phys. Rev.* **185** 500
[7] Pfistner Ch, Albers P, Lüthy W and Weber H P 1989 *Phys. Lett.* A **137** 457
[8] Chen X and Di Bartolo B 1993 *J. Lumin.* **54** 309
[9] Chen X and Di Bartolo B 1994 *J. Appl. Phys.* **75** 1710
[10] Sarkisov S E, Pukhov K K, Kaminskii A A, Petrosyan A G and Butaeva T I 1989 *Phys. Status Solidi* a **113** 193
[11] Hoshina T, Imanaga S and Yokono S 1977 *J. Lumin.* **15** 455

[12] Auzel F, de Sá G F and de Azevedo W M 1980 *J. Lumin.* **21** 187
[13] van Vliet J P M and Blasse G 1990 *J. Solid State Chem.* **85** 56
[14] Galczyński M and Stręk W 1991 *J. Phys. Chem. Solids* **52** 681
[15] Galczyński M, Blażej M and Stręk W 1992 *Mat. Chem. Phys.* **31** 175
[16] Meijerink A, De Mello Donegá C, Ellens A, Sytsma J and Blasse G 1994 *J. Lumin.* **58** 26
[17] De Mello Donegá C, Meijerink A and Blasse G 1994 *J. Lumin.* **62** 189
[18] McCumber D E and Sturge M D 1963 *J. Appl. Phys.* **34** 1682
[19] Imbusch G F, Yen W M, McCumber D E and Sturge M D 1964 *Phys. Rev.* **133** 1029
[20] Kushida T and Kikochi M 1967 *J. Phys. Soc. Japan* **23** 1333
[21] Burns G, Geiss E A, Jenkins B A and Nathan M I 1965 *Phys. Rev.* **139A** 1687
[22] Henry M O, Larkin J P and Imbusch G F 1976 *Phys. Rev.* B **13** 1893
[23] Castelli F and Lorster L S 1975 *Phys. Rev.* B **11** 920
[24] Choy T L and Yeung Y Y 1990 *Phys. Status Solidi* b **161** K107
[25] Kisliuk P, Chang N C, Scott P L and Pryce M H L 1969 *Phys. Rev.* **184** 367
[26] Laurence N, McIrvine E C and Lambe J 1962 *Phys. Chem. Solids* **23** 515
[27] van der Ziel J P 1971 *Phys. Rev.* B **4** 2888
[28] Vink A P, de Bruin M A, Roke S, Peijzel P S and Meijerink A *J. Electrochem. Soc.* submitted
[29] Di Bartolo B 1968 *Optical Interactions in Solids* (Wiley: New York) p 341
[30] Vink A P and Meijerink A 2000 *J. Lumin.* **87–9** 601–4
[31] Sytsma J, van Schaik W and Blasse G 1991 *J. Phys. Chem. Solids* **52** 419
[32] Ashcroft W and Mermin N D 1988 *Solid State Physics* (Int. Edition, Saunders College Publishing) p 618
[33] Heber J, Neukum J, Altwein M, Demirbilek R and Bodenschatz N 1998 *Spectrochimica Acta Part A* **54** 1557